
**AFRL-AFOSR-JP-TR-2022-0024**

# Investigation and exploitation of anomalously fast heat dissipation in diamond

**Mildren, Richard**
**MACQUARIE UNIVERSITY**
**BALACLAVA RD**
**NORTH RYDE, , 2109**
**AUS**

**05/09/2022**
**Final Technical Report**



Air Force Research Laboratory
Air Force Office of Scientific Research
Asian Office of Aerospace Research and Development
Unit 45002, APO AP 96338-5002

# REPORT DOCUMENTATION PAGE

**PLEASE DO NOT RETURN YOUR FORM TO THE ABOVE ORGANIZATION.**

| 1. REPORT DATE | 2. REPORT TYPE | 3. DATES COVERED | |
|---|---|---|---|
| 20220509 | Final | START DATE<br>20180930 | END DATE<br>20200929 |

**4. TITLE AND SUBTITLE**
Investigation and exploitation of anomalously fast heat dissipation in diamond

| 5a. CONTRACT NUMBER | 5b. GRANT NUMBER | 5c. PROGRAM ELEMENT NUMBER |
|---|---|---|
| FA2386-18-1-4117 | | 61102F |
| **5d. PROJECT NUMBER** | **5e. TASK NUMBER** | **5f. WORK UNIT NUMBER** |
| | | |

**6. AUTHOR(S)**
Richard Mildren

**7. PERFORMING ORGANIZATION NAME(S) AND ADDRESS(ES)**
MACQUARIE UNIVERSITY
BALACLAVA RD
NORTH RYDE 2109
AUS

**8. PERFORMING ORGANIZATION REPORT NUMBER**

| 9. SPONSORING/MONITORING AGENCY NAME(S) AND ADDRESS(ES) | 10. SPONSOR/MONITOR'S ACRONYM(S) | 11. SPONSOR/MONITOR'S REPORT NUMBER(S) |
|---|---|---|
| AOARD<br>UNIT 45002<br>APO AP 96338-5002 | AFRL/AFOSR IOA | AFRL-AFOSR-JP-TR-2022-0024 |

**12. DISTRIBUTION/AVAILABILITY STATEMENT**
A Distribution Unlimited: PB Public Release

**13. SUPPLEMENTARY NOTES**

**14. ABSTRACT**
The primary aim to determine the cause of the anomalously-high brightness of diamond lasers was addressed early in the Project by extending our research on long-pulse pumped diamond lasers. Using pulse durations sufficiently long to obtain a quasi-steady state thermal profile, we were able to identify a thermally-induced lens in diamond for the first time when using input pump powers up to 2.5 kW. The strength of the lens was determined by measuring the evolution of beam shape as a function of output power in tandem with beam propagation model. This work showed that the lens strength was consistent with a Fourier model for heat conduction, provided that the model included appropriate correction factors that take into consideration the shape and sizes of the pump and laser modes in the diamond. This result has diminished the need to invoke
more exotic processes (such as ballistic phonons) to explain the high-power behaviour. The thermal model enabled the power scaling limits of diamond lasers to be modelled with much greater certainty, and designs for the next level of power (10 kW) to be proposed.

**15. SUBJECT TERMS**

| 16. SECURITY CLASSIFICATION OF: | | | 17. LIMITATION OF ABSTRACT | 18. NUMBER OF PAGES |
|---|---|---|---|---|
| a. REPORT<br>U | b. ABSTRACT<br>U | c. THIS PAGE<br>U | SAR | 13 |

| 19a. NAME OF RESPONSIBLE PERSON | 19b. PHONE NUMBER *(Include area code)* |
|---|---|
| JEREMY KNOPP | 315-227-7006 |

**Final Report for AOARD Grant FA2386-18-1-4117**
**"Investigation and exploitation of anomalously fast heat dissipation in diamond"**

**31 Dec 2021**

**PI information:**
Prof Rich Mildren
rich.mildren@mq.edu.au

Mailing Address:
Department of Physics and Astronomy,
Macquarie University, NSW, 2109 Australia

Phone: +61 2 9850 8965
Fax: +61 2 9850 8911

**Period of Performance:** 09/29/2018– 09/30/2021

**Original Abstract:**
Diamond Raman lasers output powers are currently more than five times higher than the calculated thermal limit indicating an anomalous mechanism at play at high power loadings. The nature of the mechanism, and the extent to which it will enable higher thermally-unaffected output, are not well understood. This project aims to elucidate beam generation at extreme power loadings, with specific attention to be focused on the dynamics of phonons responsible for heat transport. Spatio-temporal phonon populations will be measured using vibronic phonon spectroscopy (VPS) to reveal the kinetics of phonon dissipation from the laser active region and thus their role in determining the temperature profile. The new thermal models will be validated, at least in part, by demonstrating diamond Raman lasers at powers up to 10 kW. The findings will be critical for predicting the thermal and optical behaviour of power-scaled diamond Raman lasers, including the potential for direct-diode pumped high power diamond Raman lasers and their potential role in other technologies.

**Executive Summary**

The primary aim to determine the cause of the anomalously-high brightness of diamond lasers was addressed early in the Project by extending our research on long-pulse pumped diamond lasers. Using pulse durations sufficiently long to obtain a quasi-steady state thermal profile, we were able to identify a thermally-induced lens in diamond for the first time when using input pump powers up to 2.5 kW. The strength of the lens was determined by measuring the evolution of beam shape as a function of output power in tandem with beam propagation model.

This work showed that the lens strength was consistent with a Fourier model for heat conduction, provided that the model included appropriate correction factors that take into consideration the shape and sizes of the pump and laser modes in the diamond. This result has diminished the need to invoke more exotic processes (such as ballistic phonons) to explain the high-power behaviour. The thermal model enabled the power scaling limits of diamond lasers to be modelled with much greater certainty, and designs for the next level of power (10 kW) to be proposed.

Armed with this improved understanding of high diamond laser operation, two major opportunities to maximize project pay-off were explored. These are summarized as follows:

> High power visible diamond Raman lasers operating on a single longitudinal mode – We had previously established that diamond Raman lasers offer a pathway towards intrinsically single-frequency output using simple standing wave cavities. While adding an intracavity frequency-doubled element extends the output range to the visible, we have also found that it also greatly stabilizes the mode. Using a 1064 nm pump, we demonstrated a 620 nm diamond laser that was single longitudinal mode at the 30 W level. This result was then adapted to target the 589 nm Na resonance, an important wavelength for applications such as space adaptive optics. Using 1018 nm pump, a 22 W single longitudinal mode laser at 589 nm was obtained. These and other similar demonstrations highlight the advantages for the diamond Raman system in generating high power and highly coherent output at red-to-yellow wavelengths.
>
> Diamond Brillouin Lasers – The first observation of Brillouin lasing in diamond were observed prior to the Project and reported at the 2018 CLEO conference in the USA. The diamond Brillouin laser concept shares many similarities with its Raman counterpart, but with some interesting extreme features such as much lower heat load, narrower gain spectrum and the ability to synthesize mm-wave band frequencies. A dedicated table-top diamond Brillouin laser was developed that enabled demonstration of the first direct-pumped diamond Brillouin laser. This featured order-of-magnitude power increases (~11 W) compared to known previously reported Brillouin lasers. We characterized the gain spectrum and provided a first measurement of the Brillouin gain coefficient. The laser output was single longitudinal mode. We anticipate this work to lead to a new class of Brillouin laser that does not require the complications associated with acoustic guidance and has the potential benefits for high power density and coherence.

The Project has also considerably advanced our understanding of polarization in diamond Raman lasers, including a rigorous treatment of the effects of crystal birefringence on laser polarization modes. A spin-off to this work was the development of a diamond Raman laser that produces pulses that have quantum-randomized polarizations, a novel device that may find application in the field of quantum encryption or simulation. The Project has also progressed our understanding of the etching phenomenon that occurs on the diamond surface under intense short-wavelength laser fields.

The major conclusions from this work show that diamond Raman lasers are capable of kilowatt power levels, beyond which thermal effects in the diamond need to be considered. Key strengths for diamond lasers in generating single frequency output at high power have been identified using both Raman and Brillouin laser gain mechanisms. We believe that the outcomes in the area of Brillouin diamond lasers flag an exciting opportunity for a new laser class with outstanding features in thermal management, narrow linewidth output, wavelengths range and mm-wave frequency synthesis.

**Introduction**

The core aims of the Project were directed towards exploring diamond laser performance and characteristics at output powers beyond 1 kW. The Project was successful in characterizing the lens properties in diamond, which has been an important aid to designing the next phases of higher-powered devices.

**Results, Discussion, Significance and Outlook:**

**1) Characterization of thermal lensing in kW-class diamond Raman lasers** (Opt. Lett. 44(10), 2506-2509 (2019); Optics Express, vol. 15, 15232, 2020)

We investigated thermal lens effects in a diamond Raman laser operating up to 1.1 kW output power in a quasi-CW steady-state regime. The external cavity diamond Raman laser was pumped for durations 7 times longer than the thermal lens time constant. As reported in Optics Letters, the system achieved some outstanding performance characteristics including an 83% slope efficiency, and a 53% optical-to-optical efficiency for conversion from a 1.06 μm pump to the 1.24 μm first Stokes. The system used a pump $M^2 = 15$, demonstrating that efficiency is maintained at the highest levels even when using exceptionally poor quality pumps. An interesting aspect of this system was that it produced high beam quality output ($M^2 < 1.3$), even at the highest power levels, despite signs for substantial thermal lensing.

Measured characteristics in the output beam parameters as a function of output power, including beam quality factor and beam divergence after a fixed focusing lens, are compared to modelling and enabled us to track the development of a thermal lens up to 16 diopters at 1.1 kW output power.

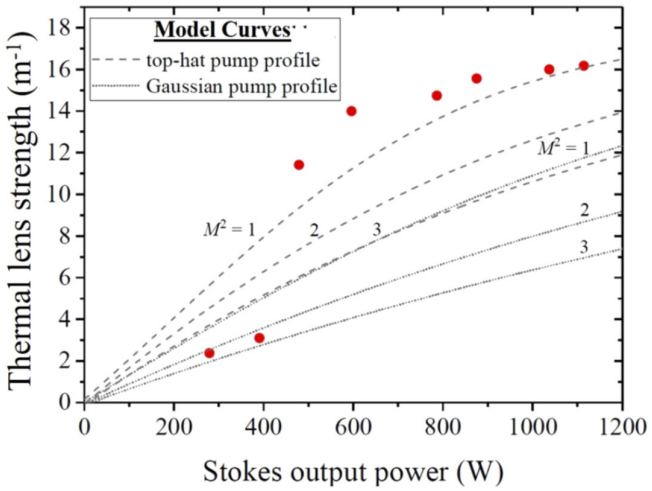


Figure 1 Thermal lens strength as a function of Stokes output power. The experimental values (red circles) use the measured $M^2$ and divergence values as input to the Stokes beam propagation calculations to determine the thermal lens strength. Model curves show two families corresponding to top-hat (dashed) and Gaussian (dotted) pump beam profiles. The pump beam profile, and the resulting power deposition profile, are deduced to have an important role on the lensing.

Analysis shows agreement between model and experiment is obtained by considering the power deposition profile and the spatial overlap with the laser mode. From a physics point of view, our work supports the Fourier heat conduction mechanism in diamond and indicates that ballistic or super-diffusive transport mechanisms (as proposed for example in Phys. Rev. 131, 2013-5, (1963)) are

unlikely to play a major role in our case. The results thus clarify aspects of our previous work that raised questions about thermal lens effects in the diamond gain medium. We now have increased confidence in our thermal models that will aid the design of continuous-wave kilowatt-class lasers or amplifiers based on single diamond elements and pumped efficiently by lasers having poor spatial coherence such as line-narrowed diode laser arrays.

**2) <u>Diamond Brillouin lasers</u>** (APL Photonics 5, no. 3, 031301 (2020))

Brillouin lasers providing extremely narrow-linewidth are emerging as a powerful tool for microwave photonics, coherent communications, quantum processors and spectroscopy. So far, laser performance and applications have been investigated for a small handful of materials and using guided-wave structures such as micro-resonators, optical fibers and chip-based waveguides. Diamond is an interesting candidate for high-power and low-threshold Brillouin lasers operating across a large range of the optical spectrum while providing frequency side bands spanning the mm-wave region.

We reported an external-cavity diamond Brillouin laser (DBL) in a bench-top bulk-optical format. Using a 5 mm-long diamond in a stabilized ring-cavity frequency-locked to the pump laser, continuous-wave lasing 167 GHz from a 532 nm pump was demonstrated using a doubly-resonant ring cavity, with a pump-limited output power of 11 W (Figure 2). Such an output power is a record for Brillouin lasers to our knowledge. The previous highest powers are obtained in glass fibers for which power is typically restricted to approximately 1W by higher-order to Stokes cascading.

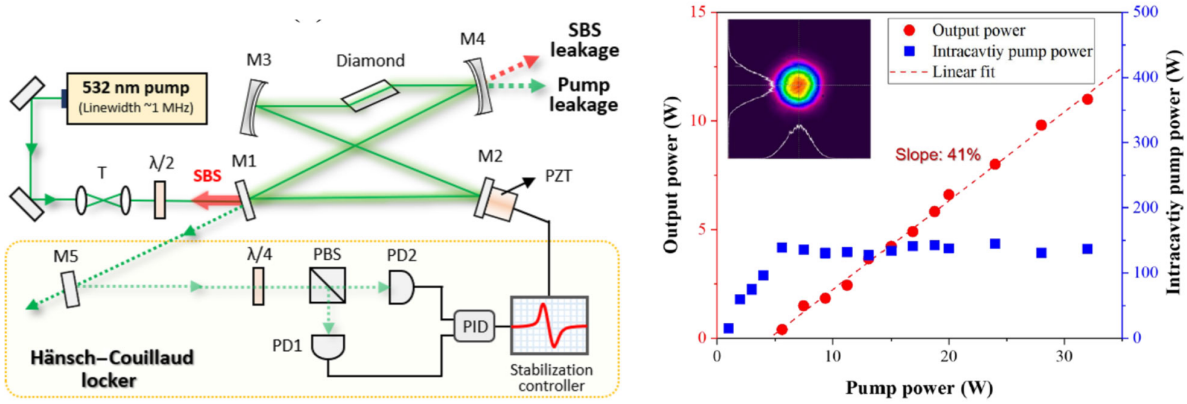


Figure 2 Layout for the free-space DBL along a plot showing the basic output characteristics.

We determined Brillouin gain coefficient to be 79 cm.GW$^{-1}$ using measurement techniques based on the laser threshold and independently from the measured linewidth and the published photoelastic coefficients. The gain linewidth of 12 MHz was obtained via a mode scanning technique. To our knowledge, these are the first reported direct measurements for these important material parameters. These Brillouin properties of diamond, along with an exceptionally high Brillouin frequency, make diamond Brillouin lasers a promising high-power source of narrow-linewidth output and mm-wave beat notes.

**<u>3) Single longitudinal mode (SLM) Raman Lasers</u>** (Optics Letters vol. 45, 1898-1901 (2020); Optics Letters vol. 45, 1898-1901 (2020))

With the high-power handling capability of diamond, and our recent developments in intrinsically-stable single frequency Raman lasers (Optica 2016), we sought to use these features to demonstrate high-power single-frequency diamond Raman lasers. Since the Raman gain provides a homogeneous

gain profile (when the pump is narrowband) and sidesteps destabilization by spatial-hole burning, there is an opportunity to develop simple standing-wave SLM lasers. By including intracavity second harmonic generation (SHG), the prospects for additional stability were increased while at the same time providing a practical path to address visible or UV laser applications requiring high coherence.

To this end, we investigated the output spectral characteristics of an intracavity SHG diamond Raman laser at the mult-ten-watt level. SLM operation of a 620 nm diamond Raman laser was demonstrated in a standing-wave cavity that included a lithium triborate second-harmonic generation element. We observed a collapse in the Stokes spectrum to SLM as the intracavity harmonic phase-matching conditions are optimized (Figure 3), enabling much higher SLM output powers to be achieved than before (by factor 10). Using a multilongitudinal mode 1064 nm Nd:YAG pump laser of power 321 W and linewidth 3.3 GHz, SLM powers of 38 W at 620 nm and 11.8 W at 1240 nm were obtained. We reported for the first time, to the best of our knowledge, an SLM Raman laser pumped using a multi-longitudinal mode input and hence a pathway for Raman lasers to provide large increases in spectral power density. The published article in Optics Letters relating to this work was flagged as an "Editor's Pick".

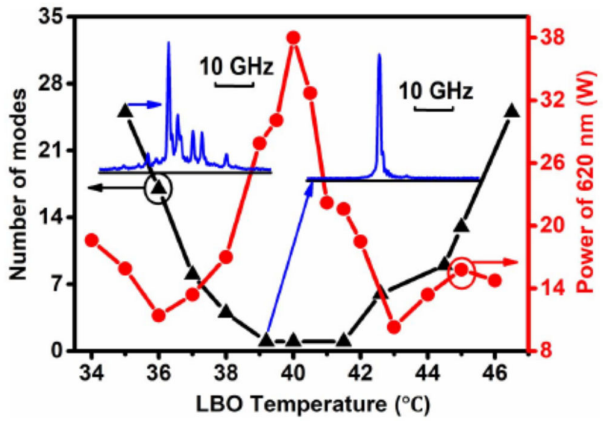


Figure 3 Collapse of the Stokes mode spectrum as the second-harmonic element is brought onto phase-matching. A maximum single-frequency output power of 38W was obtained at 620 nm (0.2 ms pulses).

The results indicate that simple standing-wave oscillators pumped by multimode Yb or Nd pumps comprise a promising practical route towards the generation of high-power SLM beams in the yellow–red part of the spectrum. Hence we also adapted the work to address a notorious problem in developing high power single frequency lasers at the Na resonance wavelength at 589 nm. A 21.7 W continuous-wave 589 nm laser with near diffraction-limited beam quality generated in a standing-wave diamond Raman resonator with intra-cavity SHG is demonstrated for the first time, to the best of our knowledge. The pump was a 1018 nm Yb-doped fiber laser with an 8 GHz spectral linewidth, comprised of an oscillator with fiber-Bragg grating mirrors and a one-stage power amplifier. The conversion efficiency from the pump to yellow was 34.4%, and 18.4% for conversion from diode at 976 nm to yellow. The measured linewidth of the SLM output at 589 nm was 8.5 MHz. By varying the temperature of the fiber-Bragg gratings from 10 to 40 °C, the SLM Stokes was tuned from 1177.945 nm to 1178.386 nm so that the SHG wavelength was tuned across the sodium D2a and D2b transition lines. One incarnation of the system is shown in the photograph of Figure 4.

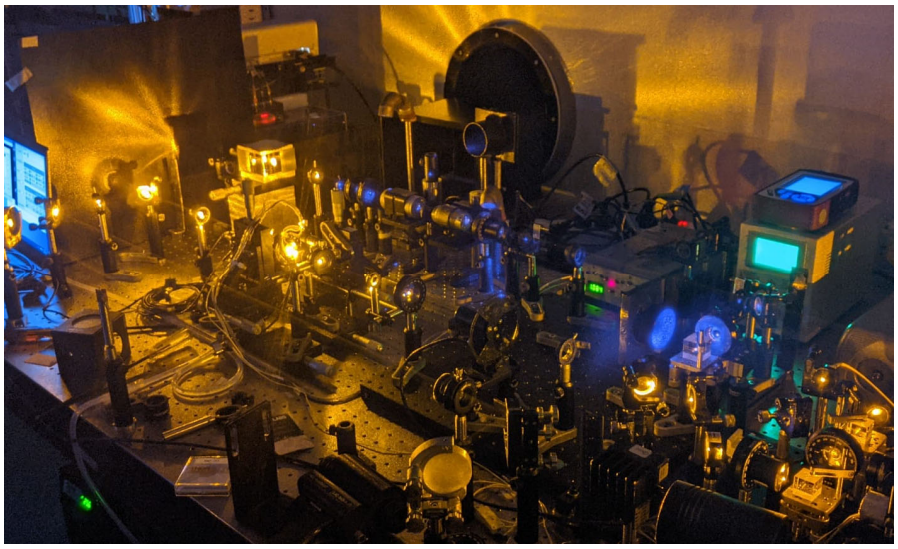

Figure 4 Photograph of the 589 nm test laser setup. Note that scattered light from the input pump beam line appears as blue in the image.

There is potential to increase laser power, achieve high average power with pulse operation and adapt the concept to other wavelengths. For narrow linewidth Raman lasers, the gain coefficient for stimulated Brillouin scattering (SBS) is often many times higher than for the Raman effect. Accordingly, SBS represents a notable parasitic effect and barrier for power scaling, a problem that notoriously afflicts high-power narrow-linewidth fiber lasers. For the example of Raman fibre guidestar lasers, which have sub-10 MHz linewidths, the maximum output powers demonstrated to date are limited by SBS despite the use of mitigation schemes and are capped at approximately 50 W. As noted above (Section 2), SBS has also been observed in diamond, but in this case it was suppressed by tuning the cavity length to avoid Brillouin resonances. Diamond laser cavities are typically hundreds to thousands of times shorter than fibre lasers; shorter cavities have larger spacings between their resonant modes so that SBS can be suppressed by selecting a cavity length for which the Brillouin wavelengths fall between resonances. For typical cavity parameters, there is a large range of cavity lengths available that avoid SBS.

The diamond laser approach thus appears to be a promising route to high power SLM operation and a method for mitigating the role of Brillouin scattering. Future suggested directions for research include power scaling, exploring lasers at other wavelengths and characterizing important features in applications such as frequency and amplitude noise. For guidestar applications, the basic laser requirement is an output wavelength matched to a narrow resonance of sodium (within the familiar yellow Na D line at 589 nm) at beam powers at least 20 W. The combination of high power and narrow linewidth presents a substantial challenge for laser developers so far met only by a few technologies and compatible with only a subset of the envisaged applications, such as night time viewing of stationary objects. A much wider range of laser performance is needed to extend applications to fast moving objects (such as low-earth orbit satellites), to increase the rate and quality of received or transmitted data (for imaging and communications), and to enable use across more of the sky and throughout the 24-hr daily cycle.

**4) Polarization dynamics in diamond Raman lasers** (Optics Express, 27(12), 17209-17220, (2019); *ibid* 29(2), 894-902, (2021).)

The residual birefringence that appears in the CVD-grown diamond crystal that we use in high power lasers potentially has a major impact on the efficiency, power and polarization properties of the laser.

We have developed a more comprehensive theory based on a Jones formalism to calculate polarisation modes in lasers containing non-collinear anisotropic gain and birefringent axes. The model describes 3 main regimes: 1) A high gain regime in which linear output polarisations are observed along the high gain axis. 2) A high birefringence regime in which linear polarisations are produced in directions along the fast and slow axis depending upon which is more closely aligned to the high gain axis. 3) A transition region producing elliptical outputs when the effects of gain and birefringence are in near balance. The model also considers the role of optical rotation in the gain medium, which is found to occur in some diamond samples. In standing-wave resonators, the rotation causes an angular offset in the polarisation behaviour; however, for unidirectional ring lasers, even small amounts of optical rotation lead to elliptical output. The theory also applies to other anisotropic systems such as silicon Raman lasers (which share crystal class with diamond) and potentially inversion lasers that have a combination of strongly anisotropic gain and birefringence.

In parallel with this work, we have also discovered that a diamond Raman laser pumped in a certain orientation creates a novel quantum-random polarization generator. We developed underpinning theory to show that the results were consistent with diamond's zero-point motion spontaneously breaking the isotropic Raman gain symmetry. This occurs as a result of the high symmetry of the diamond lattice, and in particularly the presence of a triply-degenerate $F_{2g}$ Raman mode structure of the $O_h$-symmetry. This theoretical mechanism is supported by the observed filtered uniform distribution of polarization measurements and the consistency of measurement sequences with an independent identically distributed random output as established via the NIST 800-90B standard and permutation entropy tests. These macroscopic quantum-randomized polarization states are relevant to applications in which randomness natively resides in the polarization, such as in QKD and other quantum information processing protocols. We have demonstrated coherent Stokes pulses with randomized linear-polarization orientation are generated when diamond is pumped along its [110] axis. In this configuration, the presence of multiple degenerate Raman modes results in isotropic gain, preventing the linearly-polarized Stokes pulse from acquiring a deterministic orientation and is instead randomized by the zero-point motion of the crystal. Experimental polarization measurements were found to be consistent with an independent, identical distribution with an estimated entropy rate of 6.67 bits per pulse.

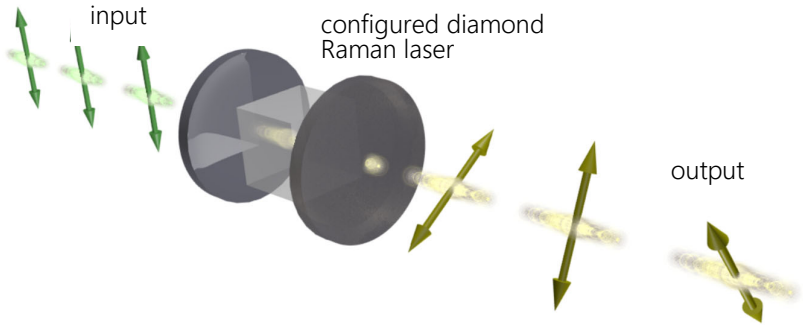


Figure 5 Concept diagram for continuous-variable quantum randomized polarization generator.

These new random states are relevant to applications where randomness is natively encoded via polarization, such as in certain quantum information processing protocols, in addition to standard applications such as quantum random number generation, simulation and machine learning where correlation-free randomness is a vital resource.

**5) Laser-induced surface phenomena** (Phys Rev. Lett., vol. 122, 016802, (2019); Appl. Phys. Lett. 117, 111601 (2020); Carbon, vol. 173, 271-285, (2020).)

Diamond is a simple substance from a lattice perspective, and has been well studied for millennia, yet it continues to reveal remarkable and unexpected phenomena. The light-induced ejection of carbon from the surfaces is such an example. UV laser-induced etching is a method of machining and nanostructuring diamond surfaces in which carbon is removed from the surface via a photochemical process involving oxygen. We have recently completed three substantial projects on the topic of UV laser interactions with the diamond surface, which are important from several perspectives including understanding laser surface damage mechanisms and as a tool to fabricate micro- or nano-sized devices.

a) Time-dependent density functional theory (TDDFT) calculations for carbon ejection

   Using a combination of atomic-scale surface characterization and TDDFT calculations, we have revealed a microscopic mechanism for carbon desorption on oxygen-terminated diamond (100) surfaces. The carbon ejection mechanism involves direct laser-induced excitation of surface carbonyl functional groups into a triply-bonded CO molecule-like state, including scission of the underlying C-C bonds. The site-specific nature of the carbon-removal process suggests that the desorption is highly promising for the top-down, atom-scale manipulation of diamond and other carbon-containing semiconductor surfaces.

b) The role of water vapour near the diamond surface

   We have shown that using a dry source of oxygen at pressures in the range of 0.01–1 Torr leads to a 10-fold increase in the etch rate compared to etching in atmospheric air. The enhanced etch rate is also found to be accompanied by a marked change in the nanopatterned surface morphology. We developed a rate equation model for the etch rate that provides good agreement with measurements for pressures up to approximately 0.1 Torr. For higher pressures, the reduced etch rate and departure from the model are attributed to the contamination of the diamond surface by trace amounts of water vapor, introduced as an impurity from the gas sources. The results provide a method for markedly increasing the etch rate, as well as a better understanding of the role of gas impurities on the etch mechanism.

c) Study of nanopattern formation as a function of surface lattice symmetry and laser polarization

   A remarkable property of UV diamond etching is the formation of nanopatterns on the surface, but the physics behind the etching as well as the pattern formation is poorly understood. To characterize the process in more detail, nanopatterns on the (100), (110) and (111) facets have been analyzed as a function of polarization, for CVD and HPHT diamond, and for nanosecond and picosecond laser pulse durations. A diverse array of behaviour is observed including sub-wavelength scale structuring with morphologies characteristic of the facet and selected polarization. As etching proceeds, the anisotropies in the quantum photon-lattice interaction are imprinted on the emergent patterns on nano and mesoscopic scales. The sum of the results leads to rules for predicting pattern type, roughness and etch rate. Supported by DFT calculations, we argue that they support a mechanism for carbon ejection based on the photo-ejection of carbonyl groups from carbonyl-supporting surfaces, defects and atomic-level step edges. The results provide guidance for optically manipulating diamond surfaces and comprise a major step towards a complete model for the process to aid laser direct-write structuring of functional diamond surfaces.

Despite these developments, there are important questions remaining. The dependence on laser wavelength and pulse duration is only partially understood. Though a mechanism for ejection has been proposed in a) above, this mechanism is yet to account for the full range of behaviour observed including the polarization dependence of nanopatterns, the etching of H-terminated surfaces, and surfaces that don't readily support carbonyl groups. Applications for the process in areas such diamond quantum devices and diamond electronics are worthy areas of future investigation.

**List of Publications and Significant Collaborations that resulted from the AOARD supported project:**

*a) Peer reviewed papers published, AOARD supported and acknowledged*


1. Xuezong Yang, Zhenxu Bai, Dijun Chen, Weibiao Chen, Yan Feng, and Richard P. Mildren, "Widely-tunable single-frequency diamond Raman laser," Opt. Express. 29(18), 29449-29457 (2021). *Open Access*

2. D.J. Little, O. Kitzler, S. Abedi, A. Alias, A. Gilchrist, R.P. Mildren, "Quantum-randomized polarization of laser pulses derived from zero-point motion of diamond" Opt. Express 29(2), 894-902, (2021). *Open Access*

3. Amanuel M. Berhane, Christopher G. Baldwin, Keri Liang, Mojtaba Moshkani, Christopher Lustri, James Downes, Catherine Stampfl, Richard P. Mildren, "Morphogenesis of mesoscopic surface patterns formed in polarized two-photon etching of diamond," Carbon, vol. 173, 271-285, (2020). *Open Access*

4. S. Antipov, R.J. Williams, A. Sabella, O. Kitzler, A. Berhane, D.J. Spence, and R.P. Mildren. "Analysis of a thermal lens in a diamond Raman laser operating at 1.1 kW output power." Optics Express 28, no. 10 (2020): 15232-15239. *Open Access*

5. C. G. Baldwin, J. E. Downes, and R. P. Mildren "Enhanced etch rate of deep-UV laser induced etching of diamond in low pressure conditions," Appl. Phys. Lett. 117, 111601 (2020) *Open Access*

6. Z. Bai, R.J. Williams, O. Kitzler, S. Sarang, D.J. Spence, Y. Wang, Z. Lu, and R.P. Mildren. "Diamond Brillouin laser in the visible." APL Photonics 5, no. 3, 031301 (2020). *Open Access*

7. X. Yang, O. Kitzler, D.J. Spence, Z. Bai, Y. Feng, and R.P. Mildren, "Diamond Sodium Guide Star Laser." Optics Letters vol. 45, 1898-1901 (2020) *Open Access*

8. O. Kitzler, D.J. Spence and R.P. Mildren, "Generalised theory of polarisation modes for resonators containing birefringence and anisotropic gain," Optics Express, 27(12), 17209-17220, (2019). *Open Access*

9. S. Antipov, A. Sabella, R.J. Williams, O. Kitzler, D.J. Spence, and R.P. Mildren "1.2 kW quasi-steady-state diamond Raman laser pumped by an M2 = 15 beam," Opt. Lett. 44(10), 2506-2509 (2019).

10. S. Sarang, O. Kitzler, O. Lux, Z. Bai, R.J. Williams, D.J. Spence, and R.P. Mildren. "Single-

longitudinal-mode diamond laser stabilization using polarization-dependent Raman gain." OSA Continuum 2, no. 4, 1028-1038, (2019). *Open Access*

11. L. Weston, J. E. Downes, C. G. Baldwin, E. Granados, S. Tawfik, X. Y. Cui, C. Stampfl and R. P. Mildren, "Photochemical etching of carbonyl groups from a carbon matrix: The (001) diamond surface," Phys Rev. Lett., vol. 122, 016802, (2019). *Open Access*

12. X. Yang, O. Kitzler, D.J. Spence, R.J. Williams, Z. Bai, S. Sarang, L. Zhang, Y. Feng and R.P. Mildren. "Single-frequency 620 nm diamond laser at high power, stabilized via harmonic self-suppression and spatial-hole-burning-free gain." Optics Letters 44, no. 4, 839-842 (2019). Editor's Pick

*b) Articles closely related to the project (funded primarily by other sources):*

1. X Yang, Z Bai, H Jiang, RP Mildren, Y Feng, "A narrow-linewidth linearly-polarized 1018 nm fiber source for pumping diamond Raman laser," Frontiers in Physics 2021

2. Muye Li, Ondrej Kitzler, Richard P. Mildren, and David J. Spence, "Modelling and characterisation of continuous wave resonantly pumped diamond Raman lasers" Opt. Express 29(12), 18427-18436, (2021). Open Access

3. D.T. Echarri, R.P. Mildren, S.M. Olaizola, and E. Granados. "Cascaded Stokes polarization conversion in cubic Raman crystals." Optics Express 29, no. 1: 291-304. (2021). Open Access

4. D.T. Echarri, K. Chrysalidis, V.N. Fedosseev, B.A. Marsh, R.P. Mildren, S.M. Olaizola, D.J. Spence, S.G. Wilkins, and E. Granados, "Broadly tunable linewidth-invariant Raman Stokes comb for selective resonance photoionization," Opt. Express 28(6), 8589-8600 (2020)

5. K. Chrysalidis, V.N. Fedosseev, B.A. Marsh, R.P. Mildren, D.J. Spence, K.D.A. Wendt, S.G. Wilkins, and E. Granados, "Continuously tunable diamond Raman laser for resonance laser ionization." Optics Letters 44, No. 16, pp. 3924-3927 (2019). Editor's Pick

6. Can Cui, Yulei Wang, Zhiwei Lu, Hang Yuan, Yue Wang, Yi Chen, Qingzheng Wang, Zhenxu Bai, and Richard P. Mildren. "Demonstration of 2.5 J, 10 Hz, nanosecond laser beam combination system based on non-collinear Brillouin amplification." Optics Express 26(25), 32717-32727 (2018)

7. S Raman Nair, LJ Rogers, DJ Spence, RP Mildren, F Jelezko, AD Greentree, T Volz and J Jeske, "Absorptive laser threshold magnetometry: combining visible diamond Raman lasers and nitrogen-vacancy centres," Materials for Quantum Technology 1 (2), 025003.

8. Z Bai, Z Zhang, K Wang, J Gao, Z Zhang, X Yang, Y Wang, Z Lu, RP Mildren, "Comprehensive Thermal Analysis of Diamond in a High-Power Raman Cavity Based on FVM-FEM Coupled Method," Nanomaterials 11 (6), 1572.

*c) A list of interactions with industry or with Air Force Research Laboratory scientists or significant*

*collaborations that resulted from this work.*

1) CERN: Dr Eduardo Granados and Dr Valentin Fedosseev
2) DST Group: Dr Alexander Sabella
3) RMIT: Prof Andrew Greentree
4) University of Sydney: Prof Cathy Stampfl
5) Shanghai Institute of Optics and Fine Mechanics: Prof Yan Feng
6) Hebei University of Technology: Prof Zhiwei Lü and A/Prof Zhenxu Bai.

*d) Invited Talks/Tutorials*

1) R.P. Mildren, "Diamond Raman Lasers" 60th Anniversary Workshop, South West Institute of Technical Phys., Chengdu, China (2018)
2) R.P. Mildren, "Diamond lasers - Challenges in commercialization" OSA Student Chapter, Nanjing (2019)
3) R.P. Mildren, "New concepts in diamond lasers" International Advanced Laser Application Summit Forum (ALAT), Shenzhen, China (2019)
4) R.P. Mildren, "Diamond Raman Lasers" Advanced Lasers and Photon Sources (ALPS2019), Yokohama, Japan (2019)
5) R.P. Mildren, "Diamond Brillouin Lasers" International Summit on Optics, Photonics & Laser Technologies, San Francisco USA (2019)
6) R.P. Mildren, "Diamond Lasers based on Stimulated Scattering" Japan Society for Applied Physics, Sapporo, Japan (2019)
7) R.P. Mildren, "Diamond Optics and Laser Lasers" Europhoton 2020, (online)

e) *Media articles*

1) Newsbreak *Laser Focus World*, April Issue: John Wallace "Diamond Brillouin laser could generate millimeter-wave frequencies for radar". https://www.laserfocusworld.com/lasers-sources/article/14169208/diamond-brillouin-laser-plus-sound-could-generate-millimeterwave-frequencies-for-nextgeneration-radar
2) AIP SciLight: Chris Patrick "Diamond Brillouin lasers provide high power, low noise" 6 Mar 2020. https://aip.scitation.org/doi/10.1063/10.0000895
3) Newsbreak *Laser Focus World*, March Issue: John Wallace "Diamond Raman laser could have higher power and efficiency for telescope adaptive optics". https://www.laserfocusworld.com/lasers-sources/article/14173385/diamond-raman-laser-could-have-higher-power-and-efficiency-for-telescope-adaptive-optics
4) Optics and Photonics News (OSA/Optica) "Diamonds: A Cryptographer's Best Friend?" by Edwin Cartlidge https://www.optica-opn.org/home/newsroom/2021/january/diamonds_a_cryptographer_s_best_friend/

**Final Comments**

Aspects of this project were affected by the COVID-19 pandemic. The main issue related to a border closure imposed by the Australian Federal Government that prevented the on-boarding of the project researcher contracted to undertake several core aspects of the Project, including plans for cryogenic

laser operation. Project progress was also impacted by temporary lab lockouts by the NSW state government. As a result, the budget and scope of the project was reduced and the emphasis altered to maximize project outcomes with the available resources. We are grateful to AOARD for a 12-month no cost extension to help alleviate these issues.